Direction of tunneling in Pb/I/$YBa_2Cu_3O_{7-x}$ tunnel junctions

A. G. Sun, A. Truscott, A. S. Katz, and R. C. Dynes
Department of Physics, University of California, San Diego, La Jolla, California 92093-0319

B. W. Veal and C. Gu
Materials Science Division, Argonne National Laboratory, Argonne, Illinois 60439
(Received 4 March 1996)

Pb/I/YBCO tunnel junctions have been fabricated on ''ab edge'' surfaces of YBCO single crystals (the ''ab edge'' surface is parallel to c axis and normal to a or b axis). The characteristics of these ab junctions were compared to those of c-axis junctions. In addition, STM studies were carried out on c-axis YBCO surfaces (studying exposed ab planes). We conclude from the combined results that the tunneling current in our previously studied c-axis junctions is along the c direction and is the result of c-axis coupling. c-axis Josephson coupling between a conventional superconductor and YBCO provides strong evidence for the existence of an s-wave component in the YBCO order parameter. [S0163-1829(96)01233-7]

I. INTRODUCTION

Despite evidence that the order parameter of high-T_c cuprates might possess $d_{x^2-y^2}$ symmetry, including several phase-sensitive experiments recently performed on YBCO,[1–3] Josephson coupling has been repeatedly observed between conventional superconductors (Pb, Sn) and YBCO along the c axis. c-axis Josephson tunneling has been observed with YBCO in the form of single crystals (twinned and untwinned) and thin films.[4–7] While the c-axis tunneling experiments do not rule out a d-wave component in the pair wave function of YBCO, they do provide clear evidence for a significant s-wave component.

Several explanations have been proposed to resolve apparent contradictions in the various experiments. One possibility is that a state of mixed s and d symmetry could occur in high-T_c superconductors as a consequence of the orthorhombicity.[8] In a second explanation, it is noted that there are Cu-O chains in YBCO in addition to the CuO_2 planes and there is growing evidence that the chains contribute to the superconductivity.[5,9,10] If the pair condensate of the chains has a component of s-wave symmetry, it provides a channel for conventional superconductors to Josephson couple into YBCO, even along the c-axis direction. This explanation is specific to the material YBCO.

A recurrent suggestion to explain the c-axis Josephson tunneling experiments is that the YBCO planar surface is not atomically flat. A bromine-alcohol etch is used to clean the surface, and this cleaning agent produces steps which provide potential tunneling channels along the ab direction (the a and b directions are mixed because of twinning). It is argued that such ab tunneling could give rise to the apparent c-axis tunneling supercurrent.

To address these issues, we have prepared junctions on ''optimally doped'' single-crystal YBCO samples with tunneling directions along both the c axis and in the ab-plane direction (normal to the c axis). This paper reports our tunneling results as well as characterization studies of the surfaces on which junctions are fabricated. To date, we have successfully fabricated ten Pb/I/YBCO (I being the insulating barrier) Josephson tunnel junctions on the crystal edges, with tunneling in the direction of the ab planes. Characteristics of these junctions were studied. Further, modulation of the Josephson current with applied magnetic field for these ''ab junctions'' leads directly to a determination of the c-axis penetration depth λ_c. Meanwhile, we have carried out STM studies of the sample surfaces of YBCO crystals that were used to fabricate our c-axis junctions. In particular, we have quantitatively investigated the steps on the c-axis surface of YBCO single crystals either as grown or caused by our etching technique, and obtained an estimate of the step wall area after successive etchings. We conclude that the step wall area is extremely small compared to the c-axis surface area, and saturates after significant etching. The STM surface characterization is presented in Sec. III. In Sec. IV, we discuss the implications of the ab junction and STM studies, and demonstrate that the supercurrent observed in our c-axis Pb/I/YBCO junctions does not originate from tunneling through step walls. In addition, we find a dependence on twin density in the Josephson coupling between conventional superconductors and c-axis YBCO. These systematics and their implications are also discussed in Sec. IV.

II. FABRICATION AND CHARACTERIZATION OF ab JUNCTIONS

The YBCO crystals used in the ab junction studies were grown at Argonne National Laboratory. The crystals were grown in gold crucibles using the conventional self-flux method.[11] Powders of Y_2O_3, $BaCO_3$, and CuO were mixed in the proportions to give the ratios Y:Ba:Cu of 5:27:68; the mixture was heated to 980 °C and cooled at rates 0.1–1 °C/h. Oxygen stoichiometries were fixed in subsequent heat treatments. Typically the samples were held for $\sim$ 4 days at 480 °C and $\sim$ 5 days at 420 °C in flowing O_2. The resulting samples were highly twinned. For these crystals, contamination from the gold crucibles results in 2–3 % of the Cu sites being substituted by Au atoms, with substitutions occurring on chain Cu sites.[12,13] Superconducting transition tempera-

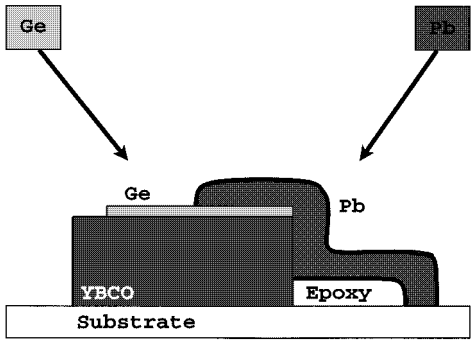

FIG. 1. Illustration of ab Pb/I/YBCO junction geometry.

tures were $\sim$ 92 K with transition widths less than 1 K. Sample thicknesses ranged from 300 to 500 micrometers, with flat rectangular edge surfaces large enough for the fabrication of ab edge junctions.

The ab junctions were made using techniques similar to those used for the fabrication of c-axis junctions.[4] First, each crystal was mounted on a glass substrate, and then etched with a solution of 1% bromine in methanol for several minutes (the etch rate is about 250 Å/min). A small amount of 5-min epoxy was spread along the bottom of the sample, covering part of the ab edge to provide a ramp for the later evaporation of a continuous Pb film (see Fig. 1). After the epoxy was cured with a 1/2 h bake at 90 °C in air, the sample was put into an evaporation chamber, and 100 Å of Ge was evaporated at an angle to cover the broad c-axis surface of the crystal, but not the crystal edge. A Pb cross stripe was then deposited across the edge surface to complete the junction. An illustration of the resulting sample is shown in Fig. 1. Like the c-axis junctions, a thin silver layer was deposited prior to the Pb deposition to reduce interdiffusion at the YBCO/Pb interface. This interdiffusion causes an undesired increase in the junction resistance. For these ab-axis junctions, a thicker silver layer (40 Å as compared to 20 Å for c-axis junctions) was necessary for the reproducible fabrication of low resistance junctions. We think this is due to either increased roughness of the edge surfaces of YBCO crystals, as revealed by STM images, or possible faster interdiffusion along the ab axis.

After the Ag and Pb evaporations, the junction was mounted on a sample stage, with leads attached for four-point measurements. The sample holder was then evacuated and quickly cooled to liquid-nitrogen temperature with exchange gas. The time period between evaporation and cooldown to 77 K was less than 1/2 h. The sample was held at liquid-nitrogen temperature before and between measurements in order to minimize degradation of the tunneling barrier with time. At higher temperatures, degradation, resulting from interdiffusion at the YBCO/Pb interface, causes the junction resistance to increase with time.

Before making measurements, the insert containing the sample was again evacuated. Using a heater mounted next to the sample stage, the sample was heated to about 120 K, well above the YBCO transition temperature. The experimental insert was then put into a liquid-helium cryostat and shielded with μ metal. The sample was cooled slowly ($\leqslant$1 K/min) through the YBCO transition temperature via a weak thermal link. After approximately 2 h, when the sample reached

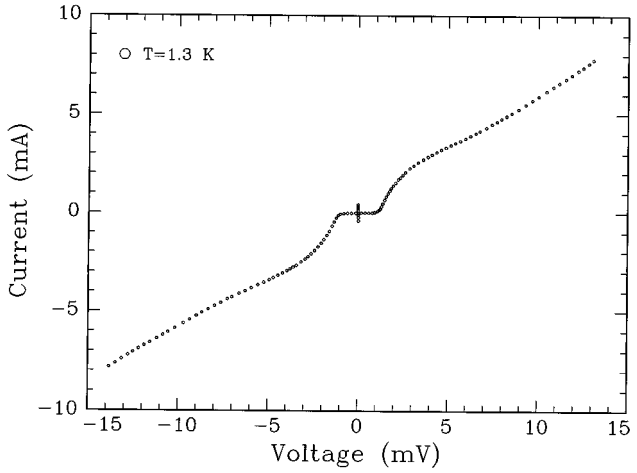

FIG. 2. Typical I-V characteristics of ab Pb/I/YBCO Josephson tunnel junctions taken at 1.3 K.

about 30 K, helium exchange gas was put into the insert to cool the sample to 4.2 K. It is our experience that this slow cooling procedure is essential for reliable Josephson measurements. It minimizes the amount of trapped flux and allows for reproducibility of the measurements.

In Fig. 2, we show the I-V characteristics of a typical ab Pb/I/YBCO junction taken at 1.3 K. The Pb energy gap is clearly visible. There is very little leakage current below the Pb gap and this attests to the quality of the tunnel junction. The quasiparticle contribution to the tunneling current is strikingly different from that observed in c-axis Pb/I/YBCO junctions. As shown in Fig. 2, there is enhanced tunneling current in the voltage range from the edge of the Pb energy gap up to about 5 mV. This corresponds to a conductance peak in the YBCO tunneling spectrum at zero bias, which is opposite to what is observed in the tunneling spectrum of c-axis Pb/I/YBCO junctions. In the c-axis case, a conductance dip is observed.[14,15] The zero-bias conductance peak has been previously reported on Pb/I/YBCO junctions made on a-axis [(100)] films.[16] In that work, the conductance peak was attributed to a spin-flip and Kondo-type scattering caused by the presence of magnetic impurities in, or near, the barrier. We consistently observe the zero-bias conductance peak in these ab junctions. Furthermore, conductance versus bias voltage curves also show that these ab junctions do not have the higher bias structures (10–50 mV) characteristic of c-axis Pb/I/YBCO tunnel junctions.[14,15]

We find that the Josephson current at zero-bias voltage varies in magnitude depending on the junction resistance, but is always present for low resistance junctions. For high resistance junctions, the Josephson binding energy is less than kT and the Josephson current is suppressed by thermal fluctuations.[17] The I_cR_n products for the ten ab junctions prepared in this study are listed in Table I. Values fall in the range 0.2–1.2 mV. c-axis tunneling measurements from the same highly twinned, Au-doped samples in this study yield I_cR_n values falling in the range 0.1–0.3 mV. The largest reported c-axis I_cR_n values were obtained from detwinned samples grown in zirconia crucibles.[5] These values ranged from 0.5 to 1.6 mV with a median value of 1 mV. Thus, I_cR_n products for our ab-axis junctions fall in the same range as the I_cR_n products for c-axis Pb/I/YBCO junc-

TABLE I. Measured values of various characteristics of ten *ab* Pb/*I*/YBCO Josephson tunnel junctions, together with corresponding values of *c*-axis junctions; the numbers in column *V* can be taken as measured values of λ_c for YBCO because $\lambda_{Pb}+t \ll \lambda_c$.

	I_c (mA)	R_n (Ω)	I_cR_n (mV)	$\lambda_c+\lambda_{Pb}+t$ (μm)	A (cm^2)	I_c/A (A/cm^2)	R_nA (Ω cm^2)
1	0.17	7.04	1.20				
2	0.019	27.0	0.51	3.8	17.2E-4	0.011	464E-4
3	0.17	6.00	1.02	2.8	14.4E-4	0.12	87.6E-4
4	0.022	8.00	0.17	0.91	2.12E-4	0.10	17.0E-4
5	0.0825	11.4	0.94	0.24	1.27E-4	0.65	14.5E-4
6	0.65	0.90	0.59				
7	0.50	1.80	0.90	0.58	0.96E-4	5.2	1.73E-4
8	0.107	3.30	0.35	1.3	0.69E-4	1.6	2.28E-4
9	0.014	12.5	0.18	1.7	3.75E-4	0.037	46.9E-4
10	0.516	2.35	1.21	0.39	5.00E-4	1.0	11.8E-4
Untwinned							
c-axis junctions	0.5–1.6	1.0	0.5–1.6		5.0E-4	1–3.2	5 .0E-4
Twinned							
c-axis junctions	0.1–0.9	1.0	0.1–0.9		5.0E-4	0.2–1.8	5.0E-4

tions prepared on single crystals. Note that smaller I_cR_n products (0.01–0.1 mV) were obtained from junctions prepared on heavily twinned thin films.[6]

We now consider the magnetic field dependence of I_c on the *ab*-axis junctions. We apply the magnetic field parallel to the *ab* plane (parallel to the sample edge) and perpendicular to the direction of tunneling, so the screening supercurrent in YBCO is flowing primarily in the *c*-axis direction. For a conventional uniform junction in the small junction limit with no trapped flux, the $I_c(B)$ curve is a Fraunhofer pattern, $I_c=I_0\left|(\sin\pi\Phi/\Phi_0)/(\pi\Phi/\Phi_0)\right|$, where I_0 is the maximum Josephson current, Φ_0 is the flux quantum, and Φ is the flux enclosed in the area defined by $[w(\lambda_{Pb}+\lambda_{YBCO}+t)]$. With known values of barrier thickness $t(\sim 20$ Å), junction width w and the penetration depth λ_{Pb} of Pb, we can obtain λ_{YBCO}. Because the dominant screening current in YBCO is flowing along the *c* axis with negligible corrections, λ_{YBCO} is the *c*-axis penetration depth λ_c.

The critical current versus applied magnetic field, $I_c(B)$, curves that we obtain on these *ab* junctions do not follow the typical Fraunhofer pattern that we observe for *c*-axis tunneling. They vary markedly from junction to junction. Some junctions, such as shown in Figs. 3(a) and 3(b), showed a double periodicity in the $I_c(B)$ curves. Other junctions, such as that pictured in Fig. 3(c), show $I_c(B)$ curves which more closely resemble the shape of the conventional Fraunhofer pattern. However, the periodicity obtained from Fig. 3(c) would correspond to a junction width smaller than that defined by geometry, taking previously reported values of λ_c.[18,19]

Unlike *c*-axis junctions, the *ab* junctions typically do not have a uniform current distribution throughout the apparent junction area. This can be determined since the $I_c(B)$ pattern corresponds to the Fourier transform of the current distribution inside the junction. A Fourier analysis reveals that the double periodicity in Figs. 3(a) and 3(b) was caused by a SQUID-like current distribution within the junction area [see inset of Figs. 3(a) and 3(b)]. For SQUID-like junctions, the two different periodicities observed in the $I_c(B)$ pattern correspond to two different length scales of the current distribution. The smaller period ΔB_1 corresponds to the distance *d* between the two current peaks: $\Phi_0/\Delta B_1=d(\lambda_{Pb}+\lambda_{YBCO}+t)$, while the larger period ΔB_2 corresponds to the width *w* of each current peak: $\Phi_0/\Delta B_2=w(\lambda_{Pb}+\lambda_{YBCO}+t)$. If we assume that *d* is approximately the geometric width of the junction, we can get an estimate of the value of λ_c for YBCO. This yields a value of λ_c on the order of 1 μm. If we now impose the condition that $(\lambda_{Pb}+\lambda_c+t)=1$ μm, we can calculate *w* for each of the junctions. This should give a measure of the actual width of the current distribution, from which we can calculate the Josephson current density of the *ab* junctions in the region where the current is flowing. Characteristics of the measured *ab* junctions are listed in Table I. We caution that rough assumptions were made in determining these junction properties; the derived numbers in Table I should be regarded as order of magnitude estimates.

For most of our *ab* junctions, the $I_c(B)$ curves were reproducible after thermal cycling following the slow cooling procedure. In general, however they are not fully symmetric in *B*. In particular, in junctions that showed SQUID-like behavior, the central peak was significantly displaced from zero field, as is evident in Fig. 3(a). In an extreme case, as shown in Fig. 4, the $I_c(B)$ curve is close to a relative minimum at zero field. Figure 4 is a close up view of Fig. 3(b) around zero bias. The minimum at zero bias corresponds to a phase shift of π between the two arms of the SQUID. This is due to the effect of trapped flux in the loop defined by two different current paths.

We can demonstrate the effect of trapped flux in *c*-axis Pb/*I*/YBCO junctions with the flux intentionally trapped in the Pb. Figure 5 shows the $I_c(B)$ pattern of a *c*-axis Pb/*I*/YBCO junction cooled through the Pb transition temperature in an applied magnetic field to produce trapped flux. Also shown in Fig. 5 is the $I_c(B)$ pattern of the *same junction* after thermal cycling through the Pb transition temperature in zero field. The trapped flux was expelled and a Fraunhofer-like $I_c(B)$ pattern was observed. For *ab* junc-

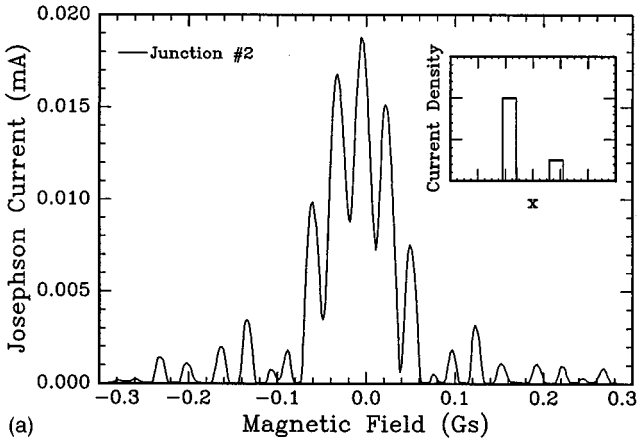

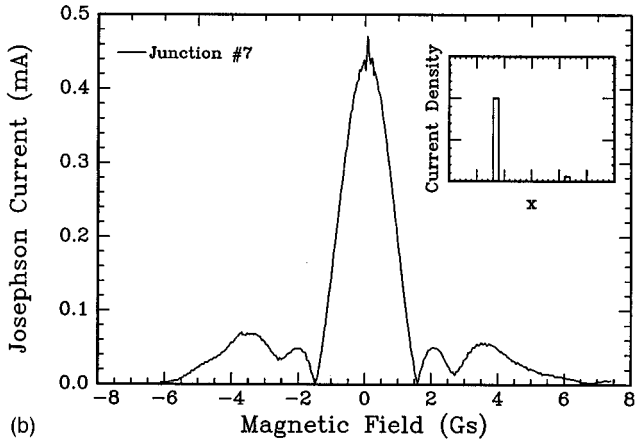

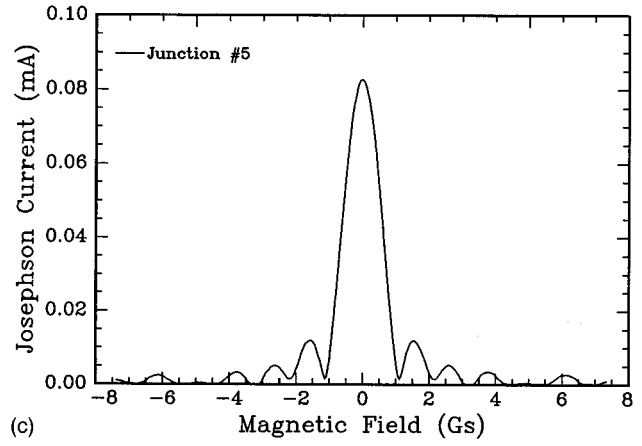

FIG. 3. $I_c(B)$ curves of three ab Pb/I/YBCO Josephson tunnel junctions, taken at 4.2 K. The insets of (a) and (b) show simple current distributions that may give rise to the corresponding $I_c(B)$ patterns.

tions, however, flux was trapped in the YBCO, and we found much greater difficulty in preparing junctions that were free of trapped flux than in the case of c-axis tunneling. The relatively good reproducibility of the ab edge junction $I_c(B)$ curves suggests that flux is very easily trapped in YBCO parallel to the ab planes of the YBCO crystal and

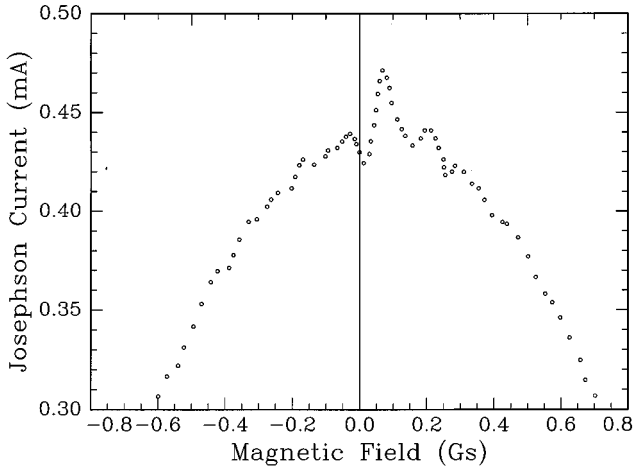

FIG. 4. Close up view of Fig. 3(b) around zero field. I_c is close to a minimum in zero field, an indication of trapped flux.

this trapping is related to the nature of the edge surface. Trapping could originate from magnetic impurities in or near the barrier, which has been shown to exist in ab junctions,[16] or it could be due to the possibility that different CuO or CuO_2 layers might have slightly different T_c's, and, as the sample is cooled down, layers with lower T_c's might trap some of the magnetic flux expelled out of the nearby superconducting layers. While we could eliminate trapped flux in our c-axis junctions, we found it difficult, if not impossible, in our ab junctions.

While trapped flux complicates most Josephson measurements (ours and others), our order of magnitude estimate of λ_c and other quantities in Table I should not be greatly affected by its presence. Reasonably good reproducibility was achieved in measurements from these junctions.

III. SURFACE MORPHOLOGY OF SINGLE-CRYSTAL YBCO

In the previous section, we demonstrated that the ab junctions show I-V characteristics that are very different from

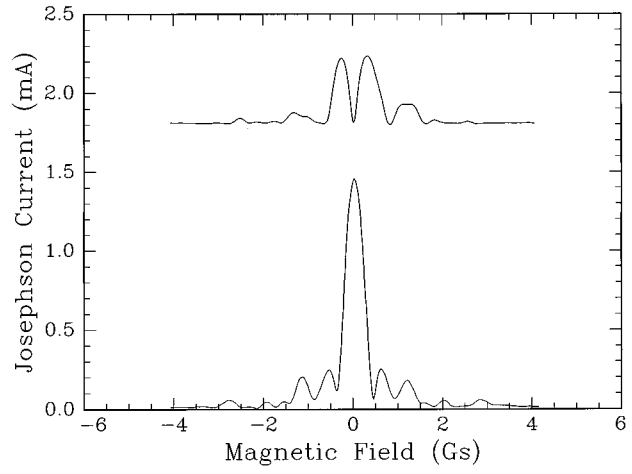

FIG. 5. $I_c(B)$ curves of a c-axis Pb/I/YBCO Josephson tunnel junction. Upper curve: with flux trapped in the Pb, and offset in y by 1.8. Lower curve: without trapped flux.

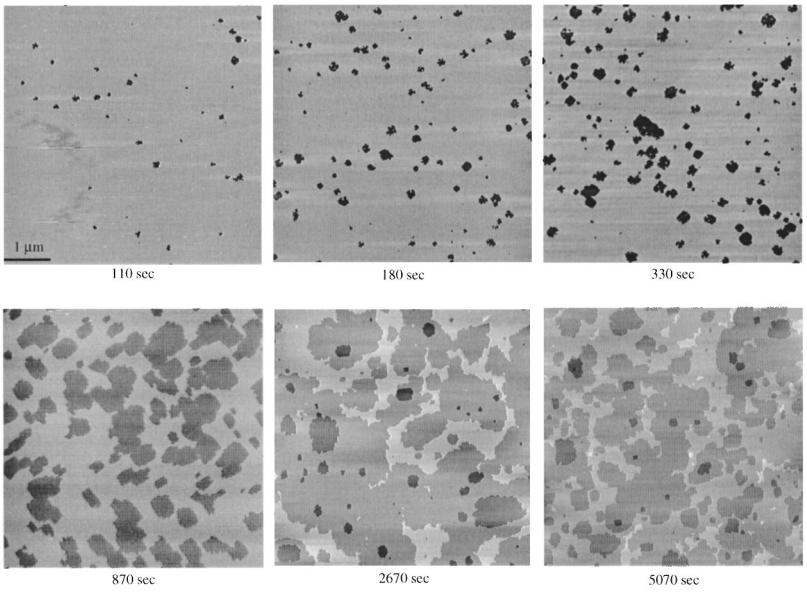

FIG. 6. STM images of a c-axis YBCO single-crystal surface. The crystal was etched in 0.5% bromine in methanol with various etch times.

those of c-axis junctions. In this section, we investigate the surface morphology of crystals on which c-axis junctions are fabricated to obtain additional information about any possible contribution to the observed Josephson current from ab-edge tunneling that might inadvertently occur from top-surface steps. In selecting crystals for the c-axis junctions, we chose ones with flat surfaces free of steps as determined using a Nomarski microscope, which is capable of detecting step heights down to 100 Å . A detailed study of surface roughening caused by the bromine etch was then carried out using scanning tunneling microscopy (STM). Single-crystal YBCO samples were scanned by STM and then successively etched and remeasured. Figure 6 shows STM pictures of a crystal surface after successive etchings. There are large atomically flat areas separated by steps. The steps on the surface revealed in these pictures were found to be a single unit cell in depth (approximately 11 Å). Further etching removes layers without increasing roughness. In other words, further etching results in the steps merging into one another, apparently, the material predominantly etches layer by layer for the etch condition we use. We have quantitatively analyzed these pictures by determining, for a series of etches, the total area of edge exposed (ab edge exposed due to the steps) as a function of etch time. This analysis is shown in Fig. 7 where we plot the ratio of exposed ab surface area to the exposed c surface area. After extended etching, the amount of exposed edge area saturates; we estimate that only 0.8% of the surface area lies in the ab edge of these steps.

The bromine etch sometimes also leaves ''etch pits'' on the c-axis YBCO crystal surface. These etch pits, visible under the Nomarski microscope, have a square geometry. Generally, they are a few tens of micrometers across and several hundred Angstroms in depth. They scatter across the c-axis surface and cluster at certain locations. The number of such etch pits varied considerably in junctions made on different crystals, from none to approximately ten over a junction area of about 0.5 mm $\times$0.2 mm. Consequently, they contribute very little additional ab surface area.

IV. DISCUSSION

We have repeatedly observed Josephson tunneling, as characterized by a well-defined Fraunhofer pattern in $I_c(B)$, in Pb/I/YBCO junctions with tunneling in the c-axis direction of YBCO. We have determined that this tunneling current cannot be attributed to ab-plane tunneling resulting from exposed steps on the sample surface. It is true that steps, approximately one unit cell in height, are introduced on the sample surface by the etchant used for preparing the surface. However, such steps constitute less than 1% of the exposed surface area. Since tunneling current density for both c-axis and edge junctions are of a similar magnitude, any contribution of ab-plane tunneling from the steps on the (c-axis) sample surface must be insignificant. Further, etch pits, typically a few tens of microns across and several hundred angstroms deep, are commonly observed. The pits can also be ruled out as a significant source of ab-tunneling current since sample surfaces can occasionally be prepared free of such pits and the usual Fraunhofer pattern is observed. Furthermore, the tunneling current does not

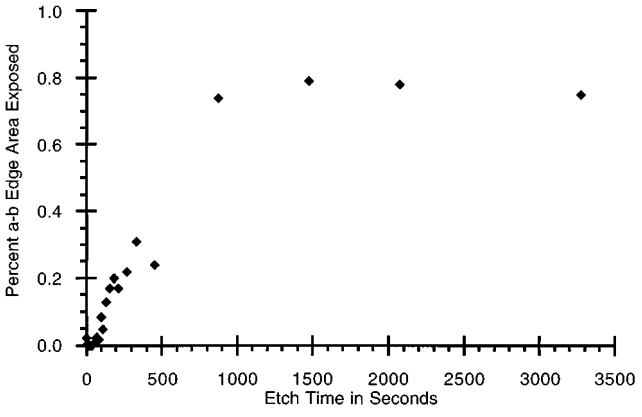

FIG. 7. The variation of exposed ab edge surface area on c-axis surface as a function of etch time with a 0.5% bromine in methanol etch.

scale with the number of etch pits, and it is hard to believe a few scattered pits can produce a uniform current distribution as evidenced by the Fraunhofer $I_c(B)$ pattern. Also, like the surface steps, the contribution of the ab-plane area from etch pits is too small to significantly contribute to the tunneling current.

An additional observation supporting the conclusion that c-axis tunneling is not significantly influenced by spurious ab-plane tunneling is provided by measurements of quasiparticle (or resistive) tunneling coming from the finite voltage characteristics. The quasiparticle tunneling shows very different behavior in the c-axis and ab junctions. The tunneling spectrum of YBCO shows a conductance dip at zero bias in c-axis junctions, but in the case of ab junctions, a zero-bias conductance peak results. This result is in agreement with previous a-axis thin-film studies.[16]

From the combination of observations: (1) well-defined and reproducible $I_c(B)$ Fraunhofer patterns of c-axis junctions that are inconsistent with ab-edge tunneling; (2) I_cR_n products, and more importantly, I_c/A (A being the junction area) and R_nA of comparable magnitudes for c-axis and ab-plane tunneling; (3) quantitative measurements of the small relative area of ab (edge) surface exposed by etching on the c-axis surfaces; and (4) dissimilar behavior of zero-bias conductance for ab and c-axis junctions, we conclude that c-axis Josephson pair tunneling is indeed measured in the observed c-axis $I_c(B)$ Fraunhofer patterns. The ab ''sidewise'' tunneling cannot account for the observed $I_c(B)$.

The Josephson tunneling is directly related to the quasiparticle tunneling. Indeed, it is the case that the I_cR_n product in conventional Josephson tunneling is well understood and in the absence of complicating circumstances (self-field effects, gaplessnesss, pair breaking, trapped flux, strong thermal fluctuations, etc.), the I_cR_n product is measured to be in agreement with the Ambegaokar-Baratoff limit.[20] It does not exceed this value. If YBCO were an isotropic s-wave superconductor obeying the BCS weak-coupling relation $\Delta=1.76k_BT_c$, the I_cR_n product for Pb/I/YBCO Josephson tunnel junctions should be about 5.2 mV. However, many observations[14] suggest that YBCO is a gapless superconductor. Even if the symmetry were strictly s wave, we would expect a reduced I_cR_n product (relative to the Ambegaokar-Baratoff limit) as a result of the gaplessness.[21]

For all of our junctions, in both c-axis and ab-plane configurations, I_cR_n products are less than the Ambegaokar-Baratoff value. Nonetheless, the c-axis I_cR_n product for detwinned crystals is substantial, about 0.5–1.6 mV suggesting a significant s-wave component in the pairing order parameter. Recall that, if YBCO were strictly a $d_{x^2-y^2}$ superconductor, we would expect the I_cR_n product to be zero (i.e., $I_c=0$).

Since the crystallographic structure of YBCO is orthorhombic, the pairing order parameter can have mixed s- and d-wave symmetry. For a superconductor with a small orthorhombic distortion, as appears in YBCO, one would generally expect a relatively pure symmetry state. However, if the electronic properties display substantial in-plane anisotropy, a more evenly mixed $d+s$ state might occur. Measurements of λ_a and λ_b performed on untwinned YBCO single crystals provide a measure of the in-plane anisotropy.[5,9,10] Since the observed anisotropy is substantial, it is reasonable to expect significant mixing of components with s and $d_{x^2-y^2}$ symmetry in the pairing order parameter. The tunneling measurements confirm the presence of an s-wave component in the pair wave function, which appears to be a significant fraction of the pair wave function in YBCO.

TABLE II. For $d+s$ pairing, the components of the order parameter that contribute to the c-axis and ab-plane tunneling for untwinned and ideally twinned crystals.

Samples	c-axis tunneling	ab-plane tunneling	Comments
Untwinned	s-wave component	b axis: $d+s$ a axis: $d-s$	Strong a-b anisotropy if $d\sim s$. Isotropic if $d\gg s$ or $s\gg d$
Twinned with $d>s$	None	d-wave component	Isotropic in ab plane
Twinned with $s>d$	s-wave component	s-wave component	Isotropic in all directions

Additional information about the order-parameter symmetry can be obtained from ab-plane and c-axis tunneling measurements on twinned and untwinned samples. Let us suppose that, within an untwinned region, the order parameter has the linear combination $d+s$ or $\Delta_d\cos2\theta+\Delta_s$, where Δ_d and Δ_s are the d- and s-wave parts of the order parameter, respectively, and $\cos2\theta=(k_x^2-k_y^2)/k^2$. Along the c-axis direction, the d-wave part is orthogonal to the s-wave conventional superconductor, e.g., Pb. Hence, c-axis tunneling on untwinned samples will give no contribution from Δ_d, but a regular contribution from Δ_s. Tunneling in the ab-axis directions will have contributions from both Δ_d and Δ_s and will reflect, in the ab plane, the anisotropy of the resultant wave function.

If we assume that the order parameter is given by a superposition of d- and s-wave functions, then we expect the conditions given in Table II for twinned and untwinned samples. We assume, for simplicity, that a twinned sample has equal areas in each twin domain orientation.

We have noted, that, for untwinned samples, c-axis tunneling measures the s-wave component; ab-plane tunneling will be sensitive to both d- and s-wave components. We expect the anisotropic $(d+s)$-wave function to be aligned with respect to an in-plane crystallographic axis (e.g., large lobes along the b axis). Thus, tunneling along this (b direction) will measure the I_cR_n product for the $d+s$ sum. The d lobes are of opposite sign in a and b directions, tunneling in the a direction will measure the I_cR_n product for $|d-s|$. Thus, if s and d components are of comparable magnitude, tunneling supercurrent will be highly anisotropic in the a-axis and b-axis directions. If d and s magnitudes are equal, pair tunneling will be maximum in one direction (b axis) and zero in the other (a axis) direction. Tunneling will be isotropic in the a and b directions if pairing is pure s wave or pure d wave.

For twinned samples, we must consider the behavior of the wave function across twin boundaries. If $\Delta_d>\Delta_s$ ($d>s$), the d-wave part of the order parameter does not change

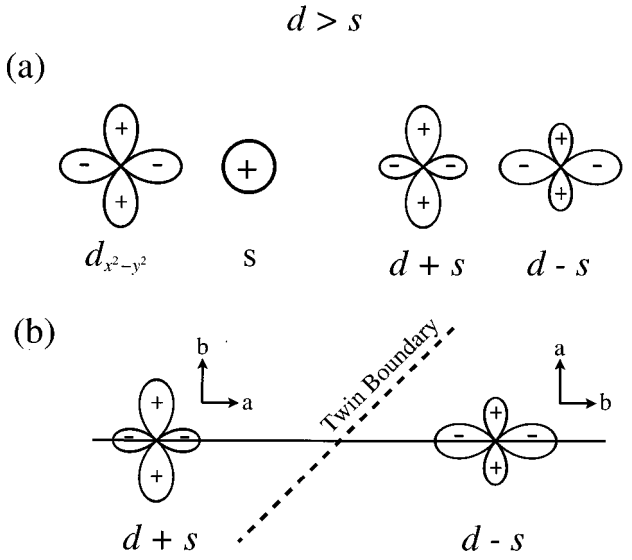

FIG. 8. A sketch of $d_{x^2-y^2}$ and s mixing with $d>s$. (a) The $d_{x^2-y^2}$ and s-wave functions as well as the combinations $d+s$ and $d-s$. (b) Proper orientation of the mixed wave function across a twin boundary.

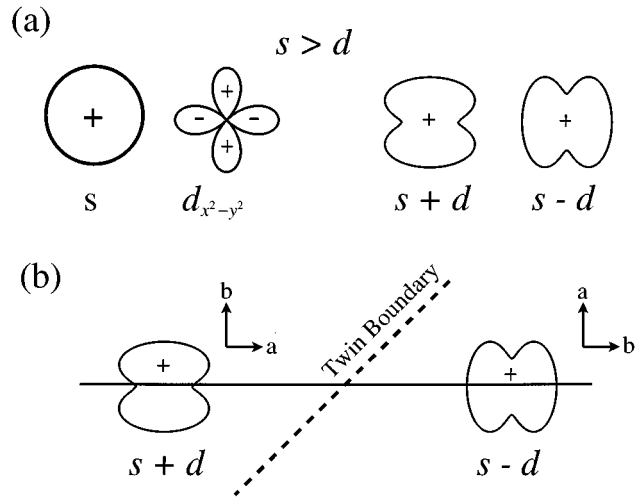

FIG. 9. A sketch of the $d_{x^2-y^2}$ and s mixing with $s>d$. (a) The $d_{x^2-y^2}$ and s-wave functions as well as the combinations $s+d$ and $s-d$. (b) Proper orientation of the mixed wave function across a twin boundary.

sign across a twin boundary,[22] the order parameter thus has the form $\Delta_d \cos 2\theta + \Delta_s$ and $\Delta_d \cos 2\theta - \Delta_s$ in adjacent domains. Figure 8(a) shows the d- and s-wave functions as well as the combinations $d+s$ and $d-s$ for the case when $d>s$. Figure 8(b) shows two adjacent twin domains. The a and b axes are interchanged at the twin boundary. Lobes of the same sign point in a given direction across the crystal while the axes of the large lobes point in the respective crystallographic directions. If equal areas of + and − twins appear within the junction, then c-axis tunneling will vanish identically since the s-wave contribution is now canceled; as usual, the c-axis d-wave contribution sums to zero. Further, the ab-plane tunneling will be purely d-wave and isotropic in the ab plane. Any c-axis tunneling current must result from an unequal distribution of + and − twin domains. Thus, we would expect the c-axis tunneling current to decrease as twin density increases; on average, the unbalanced domain area should decrease as $1/\sqrt{N}$, where N is the number of twin domains. Correspondingly, for ab-edge junctions, the tunneling will become more nearly pure d wave as the twin density increases.

For twinned samples with $s>d$, the wave function will be nodeless and $s+d$ and $s-d$ are equivalent, as shown in Fig. 9(a). Figure 9(b) shows the pair functions for two twin domains. Josephson tunneling will be purely s wave in all crystallographic directions.

We think it is premature to conclude from our Josephson tunneling measurements whether the YBCO pairing order parameter is a mixture of s and d, and if it is, which component is more dominant. However, we do make two observations. First, the I_cR_n product of ab junctions on twinned crystals appears to fall between those of twinned and untwinned c-axis junctions. Second, for the c-axis junctions, the reduction of tunneling current with increasing twin density appears to be less rapid than the $1/\sqrt{N}$ statistical distribution prediction.

We note that the assumption of statistical distribution of twinning domains may not always be suitable. When a uniaxial stress is applied to a twinned single crystal along its ab direction, domains of one orientation grow in size while domains of the other orientation shrink, until they finally disappear. Thus, for intermediate levels of stress, a very large imbalance in + and − domains might occur, even for high twin densities. Since it is not known under what conditions twins from in the crystals, we cannot be assured that increasing the twin density will tend toward equal areas of + and − twin domains. If areas are unequal, observed I_cR_n products in twinned junctions will be appropriate for a mixed twinned and untwinned sample. In this case, with $d>s$, the c-axis tunneling will not fall to zero and will not scale as $1/\sqrt{N}$. Further studies with measurements of relative areas of + and − domains are necessary

It must also be realized that tunneling results come from both thin-film and single-crystal samples which could have significant property differences in addition to the differences in twin density. We do not know if the properties of YBCO might differ from bulk properties in the vicinity of twin boundaries. Such effects might significantly alter the interpretation of the tunneling measurements. Nonetheless, a systematic dependence on twin density is clearly observed. These systematics might provide important information for quantitatively understanding the order-parameter symmetry. Present results establish that the order parameter in YBCO contains a substantial component of s-wave character.

V. SUMMARY

We have carried out a series of experiments to determine the direction of the tunneling current in c-axis Pb/I/YBCO tunnel junctions to address the concern that the observed c-axis $I_c(B)$ Josephson tunneling current might result from ab-edge steps on the sample surface. We have fabricated both ab edge and c-axis junctions on YBCO single crystals and characterized both the quasiparticle and the Josephson

tunneling current. The quasiparticle tunneling showed different characteristics in these two types of junctions. The Josephson effect was present in both types of junctions with low resistances, and both I_c/A and R_nA values fell within the same orders of magnitude. In addition, the c-axis surface of single-crystal YBCO was carefully studied using STM images. The ab step edge area was found to be only 0.8% of the c-axis area. These results strongly suggest that the tunneling current in Pb/I/YBCO junctions made on c-axis YBCO surfaces is indeed along the c axis and not a consequence of ab-edge tunneling from steps on the sample surface. The observation of c-axis Josephson coupling of Pb and YBCO gives evidence that the order parameter of YBCO has a significant s-wave component.

ACKNOWLEDGMENTS

We would like to thank Steve Kivelson, Chandra Varma, Richard Klemm, Ivan Schuller, A. P. Paulikas, and Peng Xiong for beneficial discussions, and Cathy Reddiconto for assistance with preparation of the manuscript. This work was supported by the National Science Foundation (Grant No. DMR 91-13631), the NSF Science and Technology Center for Superconductivity under Contract No. DMR 91-20000 (C.G.), the Air Force Office of Scientific Research (Grant No. F4962 092 J0070), The Office of Naval Research (ONR Grant No. N0001491J1320) and DOE-Basic Energy Sciences — Materials Sciences under Contract No. W-31-109-ENG-38 (B.V.).

[1] D. J. Van Harlingen, Rev. Mod. Phys. **67**, 515 (1995).
[2] A. Mathai, Y. Gim, R. C. Black, A. Amar, and F. C. Wellstood, Phys. Rev. Lett. **74**, 4523 (1995).
[3] J. R. Kirtley, C. C. Tsuei, Martin Rupp, J. Z. Sun, Lock See Yu-Jahnes, A. Gupta, M. B. Ketchen, K. A. Moler, and M. Bhushan, Phys. Rev. Lett. **76**, 1336 (1996).
[4] A. G. Sun, D. A. Gajewski, M. B. Maple, and R. C. Dynes, Phys. Rev. Lett. **72**, 2267 (1994).
[5] A. G. Sun, S. H. Han, A. S. Katz, D. A. Gajewski, M. B. Maple, and R. C. Dynes, Phys. Rev. B **52**, R15 731 (1995).
[6] A. S. Katz, A. G. Sun, R. C. Dynes, and K. Char, Appl. Phys. Lett. **66**, 105 (1995).
[7] R. Kleiner, A. S. Katz, A. G. Sun, R. Summer, D. A. Gajewski, S. H. Han, S. I. Woods, E. Dantsker, B. Chen, K. Char, M. B. Maple, R. C. Dynes, and John Clarke, Phys. Rev. Lett. **76**, 2161 (1996).
[8] K. Kuboki and P. A. Lee, J. Phys. Soc. Jpn. **64**, 3179 (1995); J. R. Schrieffer, Solid State Commun. **92**, 129 (1994).
[9] D. N. Basov, R. Liang, D. A. Bonn, W. N. Hardy, B. Dabrowski, M. Quijada, D. B. Tanner, J. P. Rice, D. M. Ginsberg, and T. Timusk, Phys. Rev. Lett. **74** 598 (1995).
[10] J. L. Tallon, C. Bernhard, U. Binninger, A. Hofer, G. V. M. Williams, E. J. Ansaldo, J. I. Budnick, and Ch. Niedermayer, Phys. Rev. Lett. **74**, 1008 (1995).
[11] D. L. Kaiser, F. Holtzberg, B. A. Scott, and T. R. McGuire, Appl. Phys. Lett. **51**, 1040 (1987).
[12] M. Cieplak, G. Xiao, C. Chien, A. Bakhshai, D. Artymowicz, W. Bryden, J. Stalick, and J. Rhyne, Phys. Rev. B **42**, 6200 (1990).
[13] M. Eibschutz, M. E. Lines, W. Reiff, B. van Dover, J. Waszczak, S. Zahurak, and R. J. Felder, Appl. Phys. Lett. **62**, 1827 (1993).
[14] J. Valles, Jr., R. C. Dynes, A. M. Cucolo, M. Gurvitch, L. F. Schneemeyer, J. P. Garno, and J. V. Waszcyak, Phys. Rev. B **44**, 11 986 (1991).
[15] A. G. Sun, L. M. Paulius, D. A. Gajewski, M. B. Maple, and R. C. Dynes, Phys. Rev. B **50**, 3266 (1994).
[16] J. Lesueur, L. H. Greene, W. L. Feldmann, and A. Inam, Physica C **191**, 325 (1992); M. Covington, R. Scheuerer, K. Bloom, and L. H. Greene, Appl. Phys. Lett. **68**, 1717 (1996).
[17] M. Tinkham, *Introduction to Superconductivity* (McGraw-Hill, New York, 1975), pp. 211–212.
[18] J. Schutzmann, S. Tajima, S. Miyamoto, and S. Tanaka, Phys. Rev. Lett. **73**, 174 (1994).
[19] Jian Mao, D. H. Wu, J. L. Peng, R. L. Greene, and Steven M. Anlage, Phys. Rev. B **51**, 3316 (1995).
[20] V. Ambegaokar and A. Baratoff, Phys. Rev. Lett. **10**, 486 (1963); R. D. Parks, *Superconductivity* (Marcel Dekker, New York, 1969), p. 423.
[21] I. O. Kulik, and I. K. Yanson, *The Josephson Effect in Superconductive Tunneling Structures* (Israel Program for Scientific Translation, Jerusalem, 1972).
[22] D. A. Wollman, D. J. van Harlingen, W. C. Lee, D. M. Ginsberg, and A. J. Leggett, Phys. Rev. Lett. **71**, 2134 (1993).